Journal of Solid and Fluid Mechanics (JSFM), 14(1): 1-5, 2024

Shahrood University of Technology

Journal of Solid and Fluid Mechanics (JSFM)

DOI: 10.22044/JSFM.2024.13655.3797

Manufacturing Engineering of Iran

Compiling the RN dimensionless number to determine the boundary between aerothermodynamics and radiation heating for ablative noses

Saadolahe Rostami [1], Jamasb Pirkandi [2,*], Maherdad Malekzadie deerin [3]

[1] PhD student, Department of Mechanic- Energy Conversion Engineering, Azad University, West Tehran, Iran.
[2] Assoc., Prof., Faculty of Aerospace, Malek Ashtar University of Technology, Iran.
[3] Assist, Prof., Department of Mechanic Engineering, Azad University, West Tehran, Iran.

*Corresponding author: jpirkandi@mut.ac.ir

Received: 09/26/2023 Revised: 12/23/2023 Accepted: 03/15/2024

Abstract

The most complete method to calculate aerothermodynamics and radiation heating applied to the walls of the hypersonic destructible is simultaneous solution of flow equations, chemical reaction kinetics, combustion model in the destructible layer, radiation models and flow turbulence. Using this method over time requires a high amount of computing memory. One of the effective tools for solving the flow field around various types of bodies with the stated requirements is the validated Calculating the Temperature Contores and Aero-heating (CTCA) Code. In this code used the combination of the viscous shock layer and the similarity of viscous boundary layer with the assumption that the mixed elements of the shock layer are transparent bodies. Due to the high solution time, the users of this code do not consider it reasonable to use it for preliminary design purposes. Therefore, the aim of this research is to compile the dimensionless number RN by using the results of CTCA code and Buckingham's method to determine the boundary between aerothermodynamics and Radiation heating in order to reduce the solution time related to CTCA code, So that the time to solve it for a nose with a typical flight path and cover is reduced by 15% and the maximum amount of error in the total heat flux compared to the code reaches less than 2%. It should be noted that this dimensionless number is introduced for the first time in this research.

Keywords: Combustion model, Hypersonic ablative noses, Aerothermodynamics heating, Radiation heating, Flight envelope

1. Introduction

Aerothermodynamic heating induced in different parts of the nose of supersonic payloads is caused by the conversion of kinetic energy into thermal internal energy. According to Figure 1, a large part of the thermal energy expressed is due to the Aerothermodynamic shock that leads to the creation of the shock layer, and another part of it is due to the friction of the shell and the growth of the viscous boundary layer inside the shock layer. On the other hand, the change in flight conditions (Mach number, density of the environment, etc.) causes a change in the heat flux and temperature of the shock front. So that at supersonic speeds, phenomena such as molecular Oscillatory excitations, Chemical interactions (dissociation/ionization of air and surface annihilation), the non-Isentropy of the shock layer due to the growth of the entropy layer inside the boundary layer, lead to the complicated behavior of the gas mixture of the shock layer. At temperatures lower than 1000 K, the induction of the mentioned heat flux is caused by the temperature gradient (conductive and convection heat transfer) but at higher temperatures, the gas mixture elements of the shock layer transfer a significant amount of their thermal energy in the form of radiation, which is known as Radiative heating [1]. One of the main requirements of various supersonic cargo design groups is to achieve a precise amount of heat flux. Therefore, due to the sensitivity of the subject, the discussion of heat flux is considered one of the foundations of the development of aerothermodynamics and Aerothermodynamic sciences, for this reason, the research process in this field was done by trial and error [2].

The purpose of this research is to compile and validate a dimensionless number to determine the boundary between Aerothermodynamic heating and radiation heating using the flight characteristics of cargo with Mach numbers less than 20 and using the results of the temperature contour calculation code and aerodynamic heating and Buckingham method. In such a way that by using it, it is possible to ignore Radiative heating in the range of this dimensionless number against Aerothermodynamic heating. Also,

in another range of this dimensionless number, radiation heating can be ignored against Aerothermodynamic heating.

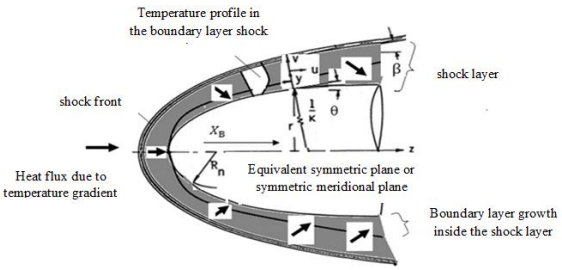

Figure 1. A view of the temperature contour of the boundary layer and the shock layer [1]

2. Equations

Due to phenomena such as air chemical interactions (dissociation/ionization) in the shock layer and surface destruction, the shock layer mixture is a mixture of different gas species. By using chemical interactions and using a combination of Miner-Lewis and Park chemical kinetic models, the instantaneous concentration of species has been calculated as one of the main inputs of the heat flux algorithm. The main inputs of these models are the instantaneous temperature and pressure of the investigated point. Therefore, these models with the equations of the viscous shock layer, the equation of state, the Baldwin-Lomax turbulence model, the species continuity equation, the energy balance equation in the decaying layer, the models for calculating the transfer properties of the species and the mixture of the shock layer (Wilk model), the heat transfer equation in the nose shell, The total heat flux equation and the radiative heating equation of gas mixture (transparent body model), shock boundary condition equations (Rangin-Hugonit model) and wall boundary condition are coupled.

3. Dimensionless Number

Using the research results [3] and [7-10], it can be said that conductive heat transfer and displacement have a direct relationship with the nose tip radius. Also, radiative heat transfer has an inverse relationship with the radius of the tip of the nose. Therefore, it can be said that the total heat flux is a function of the following variables:

$$q = \mathrm{f}(V, R, \mu, K, \rho, T, C_P, \theta)$$
$$P_1 = R(\mathrm{L})$$
$$P_2 = \mu(\mathrm{ML^{-1}T^{-1}})$$
$$P_3 = K(\mathrm{ML^{-3}\theta^{-1}})$$
$$P_4 = T(\theta) \qquad (1)$$
$$P_1' = q(\mathrm{ML^{2}T^{-3}})$$
$$P_2' = V(\mathrm{LT^{-1}})$$
$$P_3' = \rho(\mathrm{ML^{-3}})$$
$$P_4' = C_P(\mathrm{L^{2}T^{-2}\theta^{-1}})$$

In the above equations, P1, P2, P3,P4 respectively represent the radius of the nose, viscosity, conductive heat transfer coefficient and temperature of the gas mixture of the shock layer. By using Buckingham's π theorem, dimensionless groups are extracted.

4. Assumptions, Algorithm and research solution method

The assumptions of this research include the following: The flow equations in the nose are parabolic and the thickness of the boundary layer at the stagnation point is thin. Chemical interactions in the shock layer (surface destruction, dissociation/ionization of air) are unbalanced. The thermodynamic and transfer properties of the shock layer are a function of temperature, and to calculate them, curve fitting based on polar molecular theory and the results of spectroscopic experiments are used. In order to consider the effects of surface destruction, the approved theory of Park is used. Free displacement heat transfer inside the nose is equated with conductive heat transfer. Due to the high speed, the eddies caused by the turbulent flow have a two-dimensional behavior and are modeled with the Baldwin-Lomax model. Due to the high temperature of the stagnation point compared to the downstream of the flow, it is assumed that the path of radiation emission in the shock layer is from upstream to downstream of the flow. To calculate spring expressions, the time-dependent mass effect law is used. It is assumed that the gaseous environment of the shock layer is continuous, in other words, by introducing the radius of the nose as the criterion length, the Knudsen number is less than 0.001. But the numerical solution method of most of the aforementioned researches is a limited volume step by time step. Among the disadvantages of this method, we can mention the high amount of computing space and solution time And this defect will be much more pronounced in the simulation of Aerothermodynamic heating of long-range cargo during the flight path. Also, one of its advantages is the comprehensiveness of the assumption that the elements of the shock layer are absorbing and radiating due to the hyperbolic nature of the flow equations in the time-step numerical solution method. In the code for calculating the temperature contour and aerodynamic heating, in order to reduce the time of solving the flow equations, the spatial step-by-step combination method of viscous shock layer and self-

similar viscous boundary layer is used. The use of the mentioned combined method causes the flow equations to become parabolic and requires the non-distribution of information from the downstream to the upstream. That is, the requirement to use the assumption of transparency of the elements of the shock layer dictates to the designer [2] and [4-6]. In the used algorithm, we enter the input information of free flow Mach number, flight height density, nose slope and nose tip radius as CTCA code inputs in the input file of this code, and then the CTCA code is executed. Then, using the results of the code, the ratios of radiative, Aerothermodynamic heating, Lewis number, and aerodynamic and radiative heat fluxes are Calculated. The algorithm is repeated and at the end the following database is extracted. Using the output information of the algorithm, the dimensionless number (RN) is defined below. Also, the expressions Rhr and Rhc express the Radiative and Aerothermodynamic heating ratios, respectively:

$$RN = Lse = 0.286 \log\left(\frac{q}{\mu_w a_{S,w}{}^2 R}\right) = 0.286 \log\left(\frac{q_c + q_r}{\mu_w a_{S,w}{}^2 R}\right) \quad (2)$$

$$Rhr = \frac{q_r}{q} \quad Rcr = \frac{q_c}{q}$$

Using the database obtained from the solution algorithm, it was observed that:

$$\begin{cases} 2.98 \le C_1 \le 3.03 \Rightarrow C_1 \approx 3 \\ 0.20 \le C_2 \le 0.212 \Rightarrow C_2 \approx 0.206 \\ 0.025 \le C_3 \le 0.031 \Rightarrow C_3 \approx 0.028 \\ 0.69 \le C_4 \le 0.81 \Rightarrow C_4 \approx 0.75 \end{cases} \Rightarrow \quad (3)$$

$$RN = 0.286 \log\left(\frac{q}{\mu_w a_{S,w}{}^2 R}\right) = 0.286 \log\left(\mathrm{Ma}_\infty{}^3 \left(\frac{\mathrm{Re}_\infty}{\mathrm{Re}_{\infty,sl}}\right)^{0.206} 0.7^{0.028\theta^{0.75}}\right)$$

$$Rhr = \begin{cases} 0.03, \max & RN < 1 \\ 98, \min & RN > 2 \end{cases} \quad (4)$$

$$Chr = \begin{cases} 97, \min & RN < 1 \\ 0.02, \max & RN > 2 \end{cases}$$

The results obtained in equation (20) showed that:
1- In, the maximum value of Rhr is equal to 0.03, that is, the amount of radiation heating can be ignored.
2- In, the maximum value of Rcr is equal to 0.02, that is, the amount of Aerothermodynamic heating can be ignored.

5. Results and Discussion

In this section, some of the implementations carried out on the validated code for calculating the temperature contour and aerodynamic heating to extract the results obtained in "Equations (3, 4) are given under the title of case studies 1 to 4, and the results obtained in this The equations are validated with the results of reference [11]. Also, in order to introduce the amount of error caused by neglecting the heat flux in different ranges of the dimensionless number (RN), the main results of the heat flux of the validated code of calculating the temperature contour and aerodynamic heating with the secondary results of the heat flux (output of the heat flux of the validated code) Calculation of the contour of temperature and aerodynamic heating by considering the tolerance due to different ranges of dimensionless number (RN) has been compared. Related contours were introduced for quality validation. As an example, the convergence graph and execution time related to the fourth case study are shown in Figure 2, and the reduction in the convergence time of the CTCA code using the dimensionless number RN is significant.
Related contours are introduced for quality validation. As an example, the convergence graph and the execution time of a case study are shown in Figure 2, and the reduction in the convergence time of the CTCA code using the dimensionless number RN is significant.

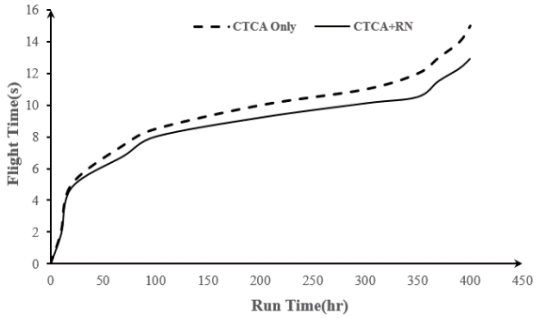

Figure 2. Effect of RN dimensionless number on CTCA code execution time in a case study

Case study (1): In this case, using the validated code to calculate the contour of temperature and aerodynamic heating, Aerothermodynamic and Radiative heating at the rest point of a parabolic nose, carbon-phenolic extinction coating and with a tip radius of 45 cm in different dimensionless numbers. (RN) was calculated (taking into account the tolerances caused by the ranges of different dimensionless numbers (RN)) and its results were compared with the results of reference [3]. This study was done to ensure the conformity of the results of the validated code for the calculation of the aerodynamic heating and temperature contour and the reference results [11] with the dimensionless number (RN).

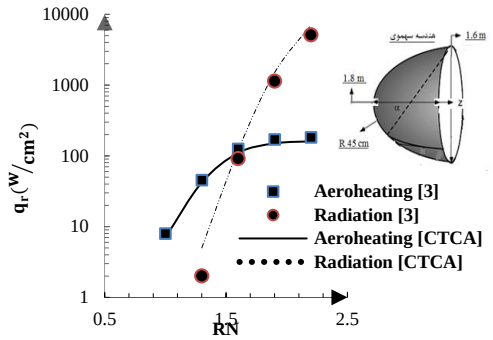

Figure 3. Comparing the results of Aerothermodynamic and radiation heating of the still point of a typical nose related to the validated code with reference [11] in terms of dimensionless number (RN)

The results of Figure 3 show that the relative error of the heat flux algorithm of the CTCA code, taking into account the amount of tolerance related to different ranges (RN), in order to calculate the thermodynamic and Radiative heating of the stagnation point, compared to reference [11], is less than 8 and 11%, respectively.

Case Study (2): In Figure 4, the radiation heating of the 0.1 model of the ship is shown with carbon-phenolic decay coating in terms of procedural distance (s) at RN=1.92, and its results are compared with reference [12] and wind tunnel test results.

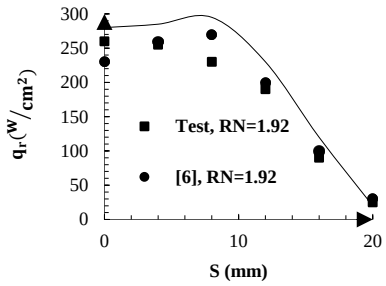

Figure 4. Radiant heating with a scale of 0.1 for the Haibasa ship in terms of distance (S) and dimensionless number 1.92

The results of "Figure 4" show that:

1-Compared to the wind tunnel test results, the curve of radiation heating changes in terms of procedural distance in the current research has a more reasonable behavior than the reference results [12].

2- The high rate of radiation heating in the points near the stagnation point in the current research compared to the results of the wind tunnel test is due to the assumption that the elements of the gas mixture are transparent.

3- The relative error of the current research and reference [12] compared to the wind tunnel test results is 10.93% and 7.2%, respectively.

Case study (3): Figure 5 shows the flight cover of a typical cargo with a nose with a geometric trestle structure and a phenolic resin-glass fiber destruction cover. Figure 8 shows the change curve of the total heat flux (conduction/displacement and radiation) meridian upwind of the nose shown in Figure 7 at an angle of attack of 10 degrees in terms of procedural distance (S) and dimensionless number (RN) and the values It is compared with the amount of Radiative heating.

Case study (3): The flight cover of a typical cargo with a nose with a geometric trestle structure and the destruction cover of phenolic resin fibers have been investigated. The changes of the total heat flux (conductive/displacement and radiation) meridian upwind of the nose were investigated. The results show that due to the low dimensionless number (RN), the amount of Radiative heating during the flight is low (less than 5% of the total heat flux).) and it can be ignored in the temperature analysis of the nose shell. It should be noted that in this case, the radiation heat flux algorithm of the validated code for calculating the temperature contour and aerodynamic heating can be disabled. Doing this reduced the time of solving the third case study by 12.3% during the flight.

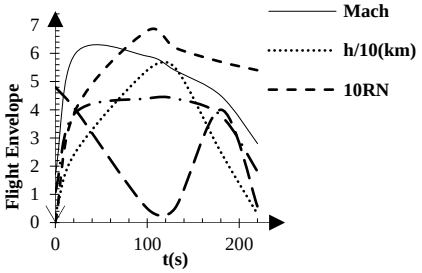

Figure 5. Flight coverage of the third case study

Case Study (4): The nose with phenolic resin-glass fiber destruction cover related to a typical cargo along with the flight cover was studied.

The results show that due to the low RN number, the amount of radiative heating during the flight is low (less than 7% of the total heat flux at t=370 sec or RN=0.9) and can be ignored in the temperature analysis of the nose shell. It should be noted that in this case, the radiative heat flux algorithm of the CTCA code can be disabled. Doing this reduced the time of solving the fourth case study by 14% during the flight.

6. Conclusions

In this research, in order to save more time in solving the validated code for calculating the temperature contour and aerodynamic heating, the overall heat flux was bounded. Dimensionless number (RN) was extracted to determine the limit of Aerothermodynamic and radiation heating. The results of these Analyzes showed that at Mach numbers less than 20, for RN<1, the amount of radiation heating can be ignored compared to Aerothermodynamic heating. Also, in RN>2, the amount of Aerothermodynamic heating can be

ignored against radiation heating. With this, depending on the value of the dimensionless number (RN), one of the Aerothermodynamic or Radiative heating subroutines can be disabled. The results of the current research for the third and fourth cases showed that the use of demarcation based on the dimensionless number (RN) saved 14 and 12.3 percent in the convergence time of the validated code for calculating the temperature contour and aerodynamic heating. It should be noted that the use of dimensionless number (RN) can also be used in engineering to estimate the total heat flux and this issue can be a good suggestion for future research following this research.

7. References

[1] J. Anderson, *Hypersonic and High Temperature Gas Dynamics*, Second Edittion, pp. 25-346, New York: ISBN: 978-964-2751-04-4. 1989.

[2] M. M. Doustar, M. Mardani, F. Ghadak, Aero-heating Modelling on the Ablative Noses during Flight Trajectory, *Aircraft Engineering and Aerospace Technology Journal*, Vol. 8, No. 3, pp.52-70, 2017.

[3] R. J. Gollan, *Numerical Modeling of Radiating Supraorbital Flows*, The University of Queensland Brisbane 4072, Australia, 2011.

[4] M. M. Doustar, M. Mardani, F. Ghadak, Simulation of temperature distribution for hypersonic ablative noses during flight trajectory by space marching method, *Modares Mechanical Engineering*, Vol. 16, No. 12, pp. 163-174, 2016 (in Persian).

[5] M. M. Doustar, M. Mardani, F. Ghadak, Investigation of the catalytic wall effect on the aerothermodynamics heating of ablative noses by space marching method, Fluid mechanic and aerodynamic *Journal of Imam hossein University*, Vol. 4, No. 2, pp. 40-50, 2019 (in Persian).

[6] M. M. Doustar, M. Mardani, F. Ghadak, Numerical simulation of radiance effects on the aerodynamic heating of ablative nose with VSL-VBLS method, *Structure and Fluid Journal of Shahrod University*, Vol. 5, No. 3, pp. 10-27, 2017 (in Persian).

[7] E.W. Miner, Computer User's Guide for a Chemically Reacting Viscous Shock Layer Code, NASA CR-2551, pp.24-32, 1975.

[8] G. Irina, C. Brykina, D. Scott, An Approximate Axisymmetric Viscous Shock Layer Aeroheating Method for Three-Dimensional Bodies, AIAA NASA, TM198-207890, pp.14-22, 1998.

[9] G.R. Dexygen1.6.1, Ablation Modeling of Nose Section with UDF Linkage to Fluent Software. *Journal of Thermophysicsand Heat Transfer*, Vol. 14, No. 3, pp. 32-41, 2012.

[10] J.D. Marvin, Turbulence Modeling for Computational Aerodynamics, *AIAA Journal*, Vol. 21, No. 7, pp. 941-955, 1983

[11] A. Kumar, Laminar and Turbulent Flow Solutions with Radiation and Ablation Injection for Jovian Entry, *AIAA Journal*, Vol. 12, No. 3, pp.30-41, 1980.

[12] D. F. Potter, Modeling of radiating shock layers for atmospheric entry at Earth and Mars, *Scientaa AC Abore*, Vol. 34, pp. 320-341, 2011.